

## MULTIVARIABLE TRANSDUCER INTERFACING CIRCUIT FOR WIRELESS MONITORING OF SMART IMPLANTS

*Sheroz Khan, A.H.M. Zahirul Alam, Zuraidah Zainudin, Muzna S. Khan, Shihab A. Hameed, Aisha Hassan Abdalla, Mohd. Rafiqul Islam*

Department of ECE (International Islamic University Malaysia), Gombak, Malaysia, sheroz@iiu.edu.my

**Abstract** – The increasing use of microprocessors and microcontrollers in measurement and data acquisition systems has necessitated the need for obtaining sensor response in a digital format, thus avoiding the need for an analog-to-digital conversion stage. Further, in quite a number of automation applications, there is the need of wireless transmission of data signals over narrow gaps. The signal obtained is loaded with data from transducers measuring parameters of interest for monitoring or other reasons. Changes in resistive sensors as a result of parameters changes are obtained as a digital signal with its time-period, amplitude and duty cycle directly proportional to variations in three different resistors. This is one useful way of reading data signals from more than a single sensors at the same time by using a measurement circuit with a single output signal. The utility of this work lies in applications where the allowable room for proper wiring is either impossible or the congestion of wiring is to be avoided for more clarity and better automation. The experimental results obtained in this paper match with the simulation details of the interface circuit.

**Keywords:** Interface Circuits, resistance to time conversion, duty cycle

### 1. INTRODUCTION

Sensors are fundamental elements in all instruments and circuits mainly applied for measurement, as well as for control of processes, both in scientific and electrical fields. They generally present analog output and can incorporate an electronic circuit to modify the output signal in order to produce a signal with suitable features for the onward stages in the hierarchy of the processes or systems.

Sensors can be resistive or capacitive-the former measure the parameter as a resistance variation while the latter measures a parameter as a capacitance variations. Both of these categories of sensors are used for applications such as for the monitoring of chemical contents in the liquid of a container, oxygen saturation in arterial or venous blood flows [1], or for detecting and assessing the health status of heart or lungs or other blood related health issues. Sensors can also be used as implanted devices such as pacers or eyeball pressure monitoring chips. These can be used in the medical industry to monitor old aged citizens in facility

homes. An example of implanted sensors can be seen in [2]. In the paper, a power harvesting microchip has been designed to provide power to and receive control signals from the implant. Once the chip is implanted, it functions as a data source to monitor the body, deriving power from external source, a technique that proves to be very useful in the medical industry, and avoiding the need of minor surgical procedures.

Another example using implanted sensors can be seen in [3] where a miniature telemetric pressure-measuring system is presented. Such telemetric systems are becoming very important in the biomedical field as interest of different biological parameters both of humans and animals is increasing.

Further examples of sensors can be seen in [4] where a sensor has been suggested for measuring the intraocular pressure (IOP) in the eye. This has proved to be an important diagnosis tool for detecting and preventing glaucoma, a disease that could lead to blindness. Another example of sensors, more towards the electrical field can be seen in [5]. In this study, a linear resistance to time converter had been employed as a detector for the soil moisture content in earth.

As can be seen from above, sensors are widely used applications that help make a circuit more useful and efficient. In our project of study, we have employed three resistive sensors. The output signal carries information on three parameters from three sources. The three features of a digital signal output varying in accordance with three parameters namely, amplitude, frequency and duty cycle. This characteristic of our circuit has been experimentally proved through simulation as well as manually through the graphs of the oscilloscope. The results matching the simulation work will be presented and discussed in details.

### 2. STATE OF THE ART WORK

As mentioned previously, our work consists of three sensors. The output signal of our circuit carries information from three different parameters. We have successfully implemented these sensors, one of them varies the time period of the output signal, the other varies the amplitude, and the last one varies the duty cycle of the output signal.

Studies concerning sensors in an electronic circuit have already been looked into, as can be seen from [6]. In this paper, a high resolution linear resistance-to-frequency

converter has been implied. The circuit consists of a Wheatstone bridge followed by an integrator and a comparator. In concept, the circuit represents a relaxation oscillator whose frequency changes linearly with the resistance change being detected by the bridge. Detection of a small resistance change is often needed in industrial and process control systems and medical instrumentation. The most sensitive means of detecting the resistance change is a Wheatstone bridge. This has been proposed in the paper mentioned above. This method is a stepping stone for our project. Our circuit consists of 3 different types of sensors. These sensors have the ability to manipulate 3 different parameters of the output signal.

Further research into the resistance-to-frequency converter can be seen in [5]. Over here the sensor has been further implied onto a soil moisture detector. An extended circuit has been added onto the circuit for the resistance-to-frequency converter. This circuit consists of LED's which light up depending on the voltage inputted to it.

Another paper of research that is related to our work is shown in [7]. A signal conditioning circuit for resistive sensors is presented. It is based on a relaxation oscillator in which both the frequency and the duty-cycle of the square-wave output signal simultaneously carry information from a pair of different sensors. The output frequency is linearly related to the resistive unbalance of a Wheatstone bridge, while the duty-cycle is independently controlled by a second sensor. This circuit can be used as an application to a thick-film pressure sensor.

The output for this circuit varies with 2 parameters namely, frequency and duty cycle. This is quite in tune with our project of study. The difference being, that we have incorporated 3 different resistive sensors rather than two. Previously, the research applied in [7] incorporated only one resistive sensor. The research paper of [3] was a further extended study of [7] because it incorporated 2 different resistive sensors. However, our area of research has further extended the study by incorporating 3 different resistive sensors. By doing so, this has given us more parameters to concentrate on.

### 3. ANALYSIS AND SIMULATION DETAILS

#### i) Amplitude Resistive Sensor

The new variable resistor lies on the feedback part of the OP AMP, the derivations below illustrate the linear relationship between the changes in resistor ( $R_y$ ) as shown in Fig.1. That voltage is equal to in magnitude and opposite in polarity to incremental voltage changes across the varying resistive  $\Delta R$ . since it is an op-amp, it can be used as a low impedance o/p point for the bridge circuit measurement.

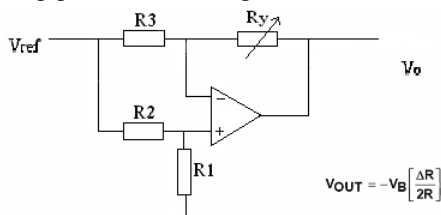


Fig. 1. Feedback Op-Amp.

$$\frac{V_i - V_n}{R3} = \frac{V_n - V_o}{R_y} \text{ ----- (1)}$$

$$V_n = V_p = V_i \left( \frac{R1}{R2 + R1} \right) \text{ ----- (2)}$$

From equations (2) and (1), we get:

$$V_o = V_i * \left( \frac{R_y R1 + R3 R1 - R_y R2 - R_y R1}{R3(R1 + R2)} \right)$$

If  $R1=R2=R3=R$  &  $R_y=R+\Delta R$  then:

$$\therefore V_o = \left( \frac{-\Delta R}{2R} \right) * V_i$$

Because the o/p is inverted and multiplied by  $\frac{1}{2R}$ , so we

need an inverter with a gain equal to 2, so that the final output  $V_{out}(t) = V_o(t)(\Delta R)/R$ ;

Where  $V_{out}(t)$  is the final o/p signal and  $V_o(t)$  is the zero crossing detector o/p voltage, so:

$$V_{out}(t) = V_o(t) * \left( \frac{-\Delta R'}{2R} \right) * (-2)$$

$$V_{out}(t) = V_o(t) * (\Delta R' / R)$$

The output voltage amplitude of the ZCD is as shown in Figure.2, which can be derived easily for a known value of resistor, R, hence calculating  $\Delta R'$ .

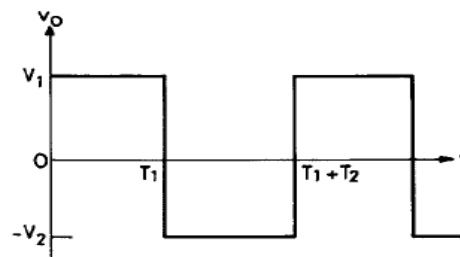


Fig. 2. Output signal across the zero crossing detector.

#### ii) Amplitude and Time Period Resistive Sensors combined

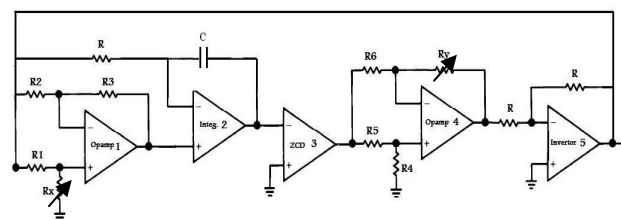


Fig. 3. Suggested circuit with output varying with two different parameters

First, the connection shown by Fig. 3 was used. The o/p of the zero crossing detector is fed to the 2nd bridge then an inverter is suggested to keep the final o/p in phase with the o/p of the zero crossing detector. From the result obtained from the simulation using Excel, its clear that the suggested connection should be modified, because the o/p of the 2nd bridge starts from zero if there is no change in  $R_y$ .

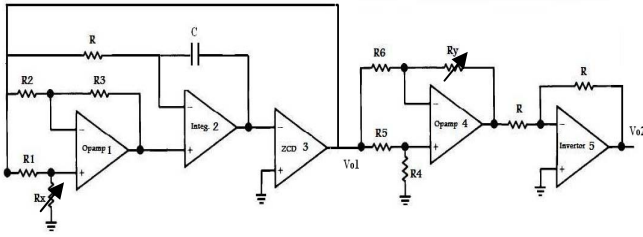


Fig. 4 Modified suggested circuit.

The Results of the circuit are shown below. These results were taken by making use of the formulas mentioned above and they were carried out using Excel tools.

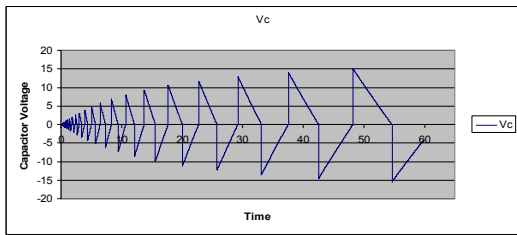


Fig. 5 Change across Vc as Rx and Ry are varied.

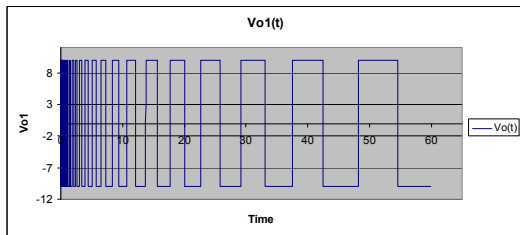


Fig. 6 Change across the Vo1 as Rx and Ry are varied.

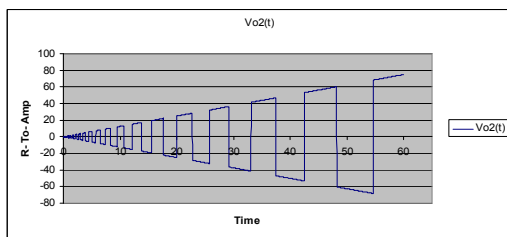


Fig. 7 Change across Vo2 as Rx and Ry are varied.

Fig. 8 below provides a theoretical linear relationship between Ry and the amplitude of the output signal. The experimental graph obtained for the same relationship will be shown later in the paper.

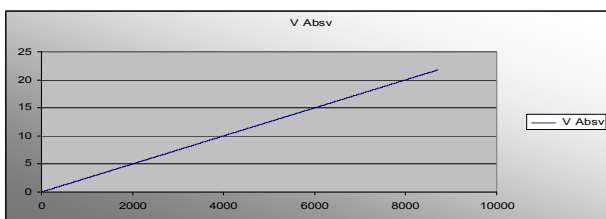


Fig. 8 Linear relationship between Ry and the amplitude of the output signal.

iii) Resistor to duty cycle circuit and its derivation:

The operational amplifier (A6) is connected to the o/p of the comparator (A3), where (A9) compares between the voltage levels produced by the change in Ry and the o/p of the integrator (A2). The circuit works as the following: the +ve part of the square wave produced by the comparator (A3) applied to the unity buffer (A6) is reflected on the o/p and C2 is charged to Vs, during the -ve half cycle the diode is off, C2 will discharge towards (A7). Hence the o/p of (A6) is approximately DC with a value equals to Vs.

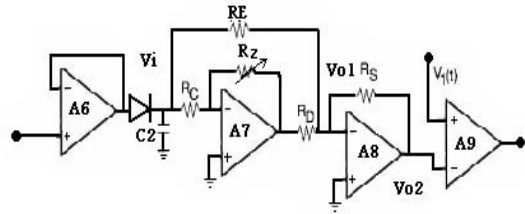


Fig. 9 Duty cycle part of the circuit.

$$Vo2 = - \left[ \frac{Rs}{RE} * Vi + \frac{Rs}{RD} * Vo1 \right]$$

$$Vo1 = - \frac{Rz}{Rc} * Vi \Rightarrow Vo2 = Vi * \left[ \frac{RzRs}{RD Rc} - \frac{Rs}{RE} \right], \text{ Where}$$

(Rz) is the varying resistor.

The suggested circuit diagram for the three –sensor scheme is shown in Fig.10.

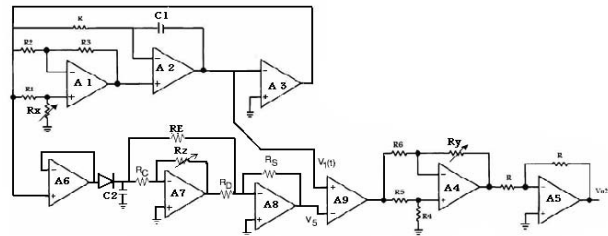


Fig. 10 Complete circuit.

Fig.11 shown below incorporates all the sensors and shows the theoretical value that has to be obtained if the circuit is to be operating perfectly. Of course the experimental output obtained will not be the same as fig. 11 because there is no means of obtaining continuously varying resistive values in a circuit that is constructed manually.

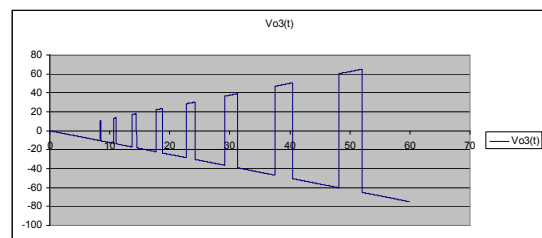


Fig. 11 Output of the circuit with three parameters varied simultaneously.

The possible range of change in  $R_z$ , which is converted into duty cycle, is limited compared to the wide range for the other two sensors. That is no surprise because the voltage of the o/p signal of the integrator is changing in a nonlinear manner and reaches some point, then it becomes fixed. Also during this time period where the integrator voltage is increasing, the duty cycle is effected by two variables rather than one. That has lead to some error in the readings.

#### 4. EXPERIMENTAL RESULTS AND DISCUSSION

To validate the proposed design, the circuit shown in Fig.10 has been bread boarded using shelf components. A LM324 was used as the zero crossing detector (A3). For the remaining amplifiers, LM741 were used. The power supply was at  $\pm 12$  V. The other relevant parameters used were that all  $R$ 's =  $4k\Omega$ ,  $C1 = C2 = 1\mu F$ ,  $R_x = R_y = R_z = 100k\Omega$  potentiometer and one 1N4148 for the diode.

To measure the response of  $R_x$ , it was varied from  $10k\Omega$  to  $140k\Omega$  while other parameters were kept constant;  $R_y=74.8k\Omega$  and  $R_z=4.8\Omega$ . For the range of  $R_x$  analyzed, Fig. 12 shows the measured time period changes when  $R_x$  was changed in  $10k\Omega$  steps, plotted in Microsoft Excel. Resistance was measured using digital multimeter, while Tektronix Digital Storage Oscilloscope was used to get the period of oscillation. Fig. 13 and Fig. 14 show the respective data recorded from the digital oscilloscope for  $R_x=10k\Omega$  and  $R_x=100k\Omega$  respectively.

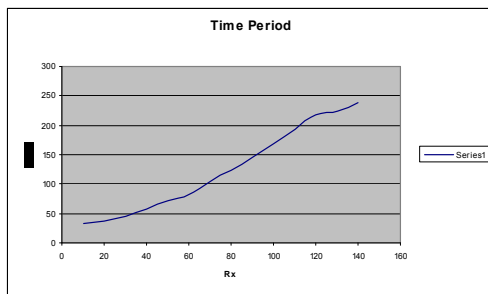


Fig. 12 Plot of experimental results for variation in  $R_x$ .

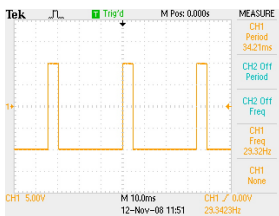


Fig. 13  $R_x = 10k\Omega$ .

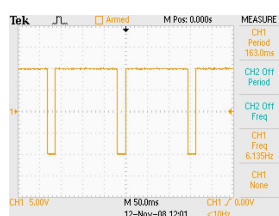


Fig. 14  $R_x = 100k\Omega$ .

The measured period output varied from  $33.42ms$  to  $238.1ms$ . The experimental results obtained were found to agree closely with the theory, where the relationship between resistance increment and time period is linear. For resistance values below than  $10k\Omega$ , unstable data were observed and hence discarded.

The same procedure was carried out to investigate the relationship between change in resistance values in  $R_y$  i.e. amplitude of the circuit output. For this,  $R_x$  value was maintained constant at  $68.1k\Omega$  and  $R_z$  at  $1.36k\Omega$ . The value for  $R_y$  was set from as low as  $0.0017\Omega$  till  $250\Omega$ . Fig. 15 shows that the output initially dropped, then started to rise at  $4.16\Omega$ , before remaining stable between  $R_y=24.43\Omega$  to  $250\Omega$ .

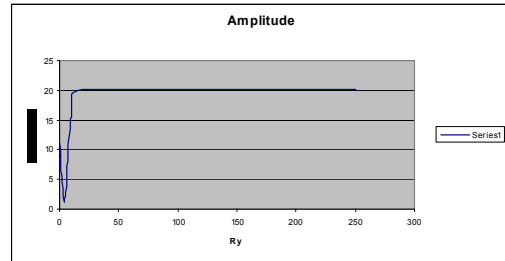


Fig.15. Plot of experimental results for variation in  $R_y$ .

This shows us that the range of our interest-for the amplitude of the output signal-is from  $4.16\Omega$  to  $24.43\Omega$ . Fig.16 and 17 below show us the change in amplitude which was shown on the oscilloscope for  $R_y$  resistance values of  $5.6$  and  $250k\Omega$ .

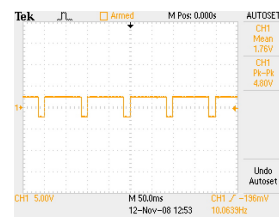


Fig.16  $R_y = 5.6k\Omega$ .

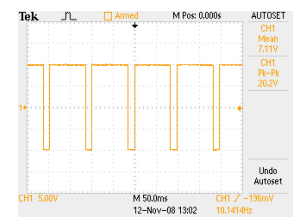


Fig. 17  $R_y = 250k\Omega$ .

During the experiment, we also observed that electrolytic capacitor caused output signal distortion and hence is not suitable to use. This is due to the fact that this specific type of capacitor is comparatively similar to the nature of a coil in construction and hence is not suitable for high-frequency circuits.

During our study, we varied the value of  $R_z$  as well. Fig. 20 below shows the graph obtained for the values of  $R_z$  and its corresponding duty cycle. The resistance value of  $R_z$  for  $1.6\Omega$  and  $5.97k\Omega$  are shown below in fig. 19 and 20.

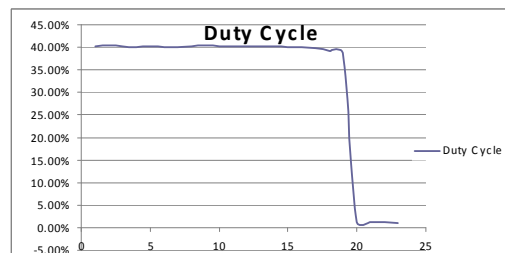


Fig. 18 Plot of experimental results for variation in  $R_z$ .

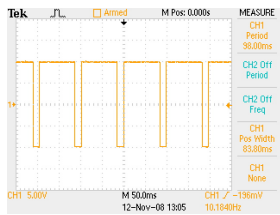


Fig. 19  $R_z = 1.6\Omega$ .

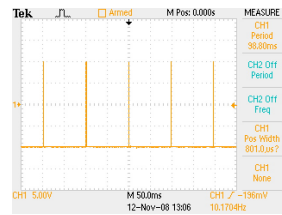


Fig. 20  $R_z = 5.97k\Omega$ .

The aim of our study was to build and analyze a circuit whereby three parameters of the output are varied using three resistive sensors. The circuit in our project was successfully constructed with three resistive parameters. This was done so for experimental purposes.

For our results, we managed to vary the relationship between  $R_x$  and the time period of the output signal. As the value of  $R_x$  increases, the time period of the output waveform also increases. These results have been shown and verified in fig. 12. Our results were obtained after quite a number of tries. We came to know that the breadboard onto which the circuit was built was very sensitive. Hence, a slight disturbance to the circuit would cause the shape of the output waveform to be disfigured. This caused us problems in acquiring results. A second problem that occurred during our research was that we could not get the proper IC for the Zero Crossing Detector. This resulted in us initially having imperfect output of the data.

It can be seen from both fig. 12 and 15 that there is a specific range where the graph is not linear. This phenomenon was observed even after the analysis was repeated several times. An acceptable reason for this would be that the circuit does not operate linearly for the complete range of  $R_x$  and  $R_y$  values. For some values, the circuit behaves abnormally. The portion of the graph in fig. 12 and 15 which do not follow a linear pattern can be treated as these values.

In conclusion to the discussion, our circuit is capable of converting resistance value ( $R_x$ ) into change of time period in the output, converting resistance value ( $R_y$ ) into change of amplitude in the output and converting resistance value ( $R_z$ ) into change in duty cycle of the output.

## 5. CONCLUSIONS

After the completion of our study and research, we can successfully conclude that we managed to achieve the desired outcomes. During our study, we wanted to test the relationship of the resistive sensors with the corresponding parameters of the output. As can be seen from the results, this has been accomplished.

The results were obtained by using Excel tools. The values for the resistance were recorded manually by using a DMM and then the corresponding output for the specific value of resistance was measured. These values were tabulated in Excel and then graphed to propose a linear relationship between the resistances and the corresponding time period of the output signal. Results from the oscilloscope have also been recorded and shown in this paper.

## REFERENCES

- [1] Meir Nitzan and Haim Taitelbaum, "The Measurement of Oxygen Saturation in Arterial and Venous Blood," IEEE Instrum. and Meas. Magazine, Vol.11, pp. 9-15, June 2008.
- [2] Christian Sauer, Milutin Stanačević, Gert Cauwenberghs, and Nitish Thakor, "Power Harvesting and Telemetry in CMOS for Implanted Devices," IEEE Trans. On Circuits and Systems, Vol. 52, No. 12, December 2005.
- [3] Stavros Chatzandroulis, Dimitris Tsoukalas, and Peter A. Neukomm, "A Miniature Pressure System with a Capacitive Sensor and a Passive Telemetry Link for Use in Implantable Applications," Journal of Microelectromechanical Systems, Vol. 9, No. 1, March 2000.
- [4] Santiago Lizón-Martínez, Romano Giannetti, José Luis Rodríguez-Marrero, and Bernardo Tellini, "Design of a System for Continuous Intraocular Pressure Monitoring," IEEE Trans. On Instrumentation and Measurement, Vol. 54, No. 4, August 2005.
- [5] Sheraz Khan, A. H. M. Zahirul Alam, Othman O. Khalifa, Mohd Rafiqul Islam, Zuraidah Zainudin, Muzna S. Khan, and Nurul Iman Muhamad Pauzi, "A High Accuracy Measurement Circuit for Soil Moisture Detection," International Journal of Mathematical, Physical and Engineering Sciences, Vol. 2, No. 2.
- [6] Kouji Mochizuki, and Kenzo Watanabe, "A High Resolution, Linear Resistance-to-Frequency Converter," IEEE Trans. On Instrumentation and Measurement, Vol. 45, No. 3, June 1996.
- [7] Vittorio Ferrari, Carla Ghidini, Daniele Marioli, and Andrea Taroni, "Oscillator-Based Signal Conditioning with Improved Linearity for Resistive Sensors," IEEE Trans. On Instrumentation and Measurement, Vol. 47, No.1, Feb. 1998.